Pis'ma v ZhETF, vol. 98, iss. 7, pp. 427 – 431 © 2013 October 10

Correlated band structure of superconducting $NdFeAsO_{0.9}F_{0.1}$: dynamical mean-field study

S. L. Skornyakov, I. R. Shein[+], A. L. Ivanovskii[+], V. I. Anisimov

Institute of Metal Physics UB of the RAS, 620990 Yekaterinburg, Russia

Ural Federal University, 620002 Yekaterinburg, Russia

[+]*Institute of Solid State Chemistry UB of the RAS, 620990 Ekaterinburg, Russia*

Submitted 1 July 2013

Resubmitted 18 August 2013

In this Letter we report the LDA+DMFT (method combining local density approximation with dynamical mean-field theory) results for spectral properties of the superconductor $NdFeAsO_{0.9}F_{0.1}$ in the paramagnetic phase. The calculated momentum-resolved spectral functions are in good agreement with angle-resolved photoemission spectra (ARPES). The obtained effective quasiparticle mass enhancement ($m^*/m = 1.4$) is smaller than the one in isostructural parent compound LaFeAsO which critical temperature under the same fluorine doping ($LaFeAsO_{0.9}F_{0.1}$) is two times lower. Our results demonstrate that in quaternary FeAs-based superconductors of the same class, changes of the crystal structure caused by substitution of one rare-earth atom, implicitly result in reduction of the electronic correlation strength.

DOI: 10.7868/S0370274X1319003X

The discovery of high-temperature superconductivity in iron-arsenic compounds [1] attracts considerable amount of attention to this class of systems from theoretical and experimental communities [2–17]. This interest is stimulated by the fact that the new superconductors are similar to well-studied cuprates. Both superconducting families adopt layered crystal structures where layers of atoms responsible for superconductivity alternate with non-conducting layers. As in the cuprates, superconductivity in the pnictides emerges under doping and parent compounds typically are not superconducting. The main difference between the two classes of superconductors is the nature of the ground state of their parent systems. In the case of cuprates it corresponds to a Mott insulator while for the pnictides it is a metal. It is well established that strong Coulomb correlations between copper electrons play a key role in formation of superconducting state in the cuprates. Thus, studying correlation phenomena in the pnictides is important for revealing the pairing mechanism in these systems.

Strength of electronic correlations in the pnictides was a central topic of numerous works [2–9]. These studies were done within the LDA+DMFT scheme [18] which is the most powerful first-principle approach that can be routinely applied to studying electronic structure of realistic strongly correlated systems. It combines the local density approximation (LDA) which describes band dispersion in real materials with the ability of the dynamical mean-field theory (DMFT) [19] to treat the whole range of on-site Coulomb correlations. First LDA+DMFT results [3] on pnictides were interpreted in such a way that these systems should be considered as strongly correlated systems close to a Mott transition. However, analysis of band dispersion carried out in later studies [4–6] have shown that it is more correct to classify the new superconductors as moderately correlated compounds.

The highest T_c in the pnictides is detected for doped systems [20, 21], therefore studying the electronic properties in the doped cases and revealing differences with the stoichiometric cases can be useful for understanding the physics of superconductivity in these compounds.

Neodymium ferrooxyarsenide is a parent compound for high-temperature superconductors with common formula $NdFeAsO_{1-x}F_x$ ($T_c = 51\,\mathrm{K}$ for $x = 0.1$ [21]). This compound is the second synthesized pnictide-based material after PrFeAsO that under fluorine doping turns into superconducting state above 50 K [21, 11] and is isostructural to other famous pnictide superconductor LaFeAsO ($T_c = 26\,\mathrm{K}$ for $LaFeAsO_{0.9}F_{0.1}$ [20]). Since substitution of La with isovalent and chemically equivalent Nd preserves the crystal lattice symmetry, electronic structures in these two cases are not expected to be qualitatively different. However, due to small difference in the ionic radii this change causes structural relaxation which results in small decrease

of the lattice parameters and reduction of the Fe–As–Fe bond angle. These changes of the crystal structure seem to be very important since critical temperatures in these two cases are considerably different. Therefore the change La→Nd influence the superconducting properties and, probably, the Fermi surface, indirectly. Interplay between the structural changes and the electron pairing in so-called "1111" systems (quaternary compounds like LaFeAsO, NdFeAsO) was studied by Kuroki et al. [12] within density-functional theory and model approaches employing random-phase approximation.

In view of the fact that transition temperatures in NdFeAsO and LaFeAsO are almost two times different it is instructive to study and compare electronic structure of these compounds. Direct probe of band dispersion and Fermi surface in real materials is provided by photoemission spectroscopy with angular resolution which requires large high-quality single crystals. Comparison of an ARPES data with calculated spectral properties allows to judge on the role and strength of electronic correlations. However, it turned out that growth of such crystals is a non-trivial task for some representatives of the "1111" family.

Electronic structures of $NdFeAsO_{1-x}F_x$ and LaFeAsO were intensively studied experimentally [13–17]. Authors of these works have shown that observed band structure of the investigated compounds in general can be interpreted as renormalized LDA bands but formation of some important features of the Fermi surface cannot be understood and within LDA. It was also noted that the surface states contribute significantly to the ARPES spectra and distinction between the bulk and the surface contributions requires separate analysis. Theoretical investigation of spectral properties of stoichiometric LaFeAsO in framework of LDA+DMFT was done by Aichhorn et al. [4] and Anisimov et al. [2]. These results are in good agreement with angle-resolved and angle-integrated spectra [13–15, 22]. Thus, first high-resolution ARPES spectra of fluorine-doped NdFeAsO were measured more than four years ago [16] and so far only few DFT-based calculations of its electronic structure without any account of strong electronic correlations were reported [16, 23].

In this work, we present the LDA+DMFT results for spectral properties of $NdO_{1-x}F_xFeAs$ and its parent system in the paramagnetic state. We demonstrate that local Coulomb correlations taken into account within single-site dynamical mean-field approach are essential for proper description of electronic structure of this compound. Our results are in good agreement with the available ARPES data. We compare our results with LDA+DMFT data for LaFeAsO.

Implementation of the LDA+DMFT scheme employed in the present work consists of three steps. First, self-consistent LDA calculation is carried out and the effective on-site Coulomb parameter U and intraatomic exchange parameter J are computed by means of the constrained DFT method [24]. In our study we calculate the LDA band structure and spectral function with ELK full-potential code [25] using the experimentally determined atomic positions [26] and default parameters controlling the LAPW basis. On the second step basis of Wannier states describing band structure in vicinity of the Fermi energy is generated and the effective tight-binding Hamiltonian $\hat{H}_{\mathrm{W}F}$ in that basis is constructed by means of projection technique [27]. Then many-body Hamiltonian $\hat{H}(\mathbf{k})$,

$$\hat{H}(\mathbf{k}) = \hat{H}_{\mathrm{W}F}(\mathbf{k}) + \hat{H}_{\mathrm{U}} - \hat{H}_{DC}, \qquad (1)$$

is iteratively solved by DMFT. On each iteration the effective DMFT impurity problem is solved by the hybridization function expansion continuous time quantum Monte-Carlo method (CTQMC) [28]. In Eq. (1) $\hat{H}_{\mathrm{U}}$ describes the on-site Coulomb interaction energy and the term $\hat{H}_{DC}$ is the correction for the Coulomb energy already accounted by LDA. In our work we used the Coulomb interaction term in the density-density form,

$$\hat{H}_{\mathrm{U}} = \frac{1}{2}\sum_{ij\sigma\sigma'} U_{ij}^{\sigma\sigma'}\hat{n}_{i\sigma}\hat{n}_{j\sigma'}, \qquad (2)$$

where $\hat{n}_{i\sigma}$ is the particle-number operator for the orbital i and spin projection $\sigma = \uparrow\downarrow$, U_{ij} is the interaction matrix which is parametrized [29] by U and J. The double-counting $\hat{H}_{DC}$ is represented by a diagonal matrix with nonzero elements in the block of partilly filled states (Fe $3d$ states in the present case). It was taken in the form $\overline{U}(n_d - 0.5)$ where n_d is the total number of electrons in partially filled shells, and $\overline{U} = \sum_{ij} U_{ij}^{\sigma\sigma'}/N(N-1)$ is the average Coulomb energy for N spin-orbitals (N=10 in the case of a d element). This form of $\hat{H}_{DC}$ can be successfully applied for modeling of spectral and magnetic properties of different FeAs superconductors [5, 6, 10].

Momentum-resolved spectral functions including effects of local electronic correlations were computed as imaginary part of the DMFT Green's function:

$$A(\mathbf{k},\omega) = -\frac{1}{\pi}\mathrm{Tr}\mathrm{Im}[(\omega+\mu)\hat{I} - \hat{H}_{\mathrm{W}F}(\mathbf{k}) + \hat{H}_{DC} - \hat{\Sigma}(\omega)]. \qquad (3)$$

Here μ is the self-consistently determined chemical potential, $\hat{\Sigma}(\omega)$ is the real-frequency self-energy obtained

by means of analytical continuation of the DMFT self-energy $\hat{\Sigma}(i\omega_n)$ (ω_n is the Matsubara frequency) with the use of Padé approximants [30] and $\hat{I}$ is the identity operator.

Comparison of spectral functions of stoichiometric NdFeAsO and LaFeAsO obtained within LDA is shown in Fig. 1. As in other pnictides in both cases Fe $3d$ states

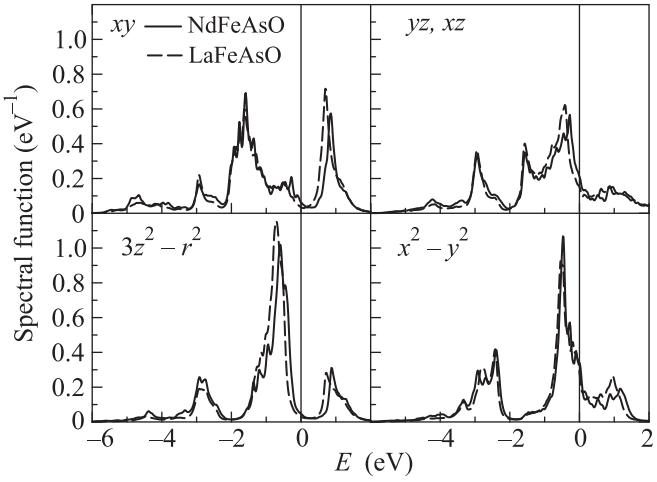

Fig. 1. Orbitally resolved spectral functions of stoichiometric NdFeAsO (solid curves) and LaFeAsO (dashed curves) calculated within LDA. 0 eV corresponds to the Fermi energy

form a broad band in the energy region $(-2.0,\ 2.0)$ eV relative to the Fermi level. Features in the energy window $(-6.0,\ -2.0)$ eV are due to Fe d – As p hybridization. Overall shape of the spectral functions computed for the two cases is similar. However, due to difference in the crystal structures, in the case of Nd-based compound position of the peaks located in the energy window $(-1.0,\ 0.0)$ eV for the yz, xz and $3z^2 - r^2$ is 0.2 eV closer to the Fermi energy. Within the LDA solution partial substitution O→F (electron doping) shifts these peaks from the Fermi level and difference in their position can hardly induce changes in low-temperature properties such as T_c.

Band structure of stoichiometric NdFeAsO computed within LDA is shown in Fig. 2. We model band structure of a doped system varying the total number of electrons. Topology of the Fermi surface of the doped system obtained within LDA has qualitative disagreement with ARPES spectrum shown in the lower panel of Fig. 3. First of all, there is no hole pocket centered at the Γ point, and the flat band on the energy −0.25 eV is also missing. In addition, depth of the electron pocket centered at the M point is overestimated. Thus, it is impossible to reproduce the experimentally observed band structure by a simple shift of the chemical potential.

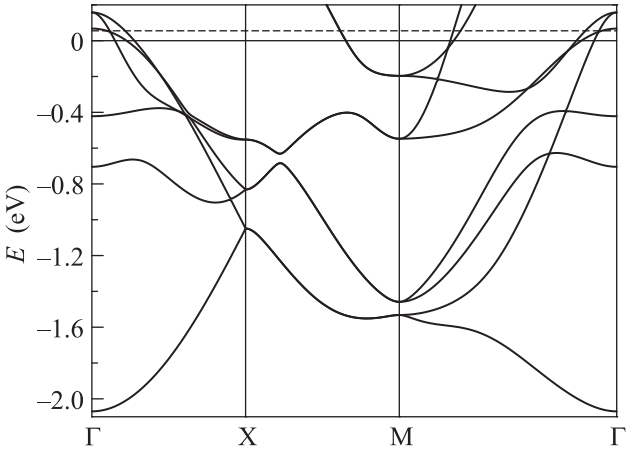

Fig. 2. Energy bands of NdFeAsO obtained in LDA for the Γ–X–M–Γ path in the Brillouin zone. The Fermi energy of the undoped system is set to 0 eV. The dashed line corresponds to the Fermi energy of the fluorine-doped compound $NdFeAsO_{0.9}F_{0.1}$

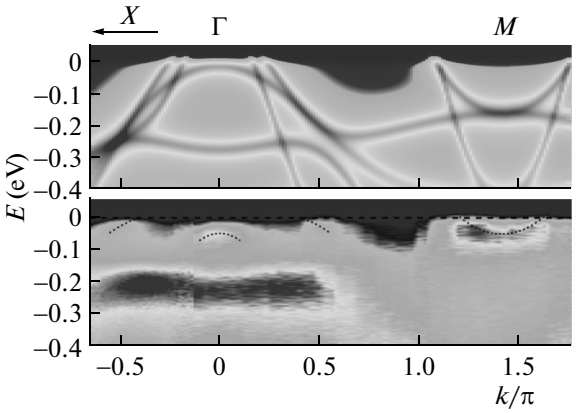

Fig. 3. The **k**-resolved spectral function $A(\mathbf{k},\omega)$ of $NdFeAsO_{0.9}F_{0.1}$ along the X–Γ–M–Γ path in the Brillouin zone visualized as a contour plot. Upper panel: the LDA+DMFT spectral function. Lower panel: the corresponding ARPES spectrum by Liu et al. [16]. The Fermi energy is set to 0 eV

Since electron correlations play an important role in the pnictides the LDA solution can be modified by explicit inclusion of the Coulomb interaction between electrons in partially filled orbitals into consideration.

In the present study we use the interaction parameters $U = 3.5$ eV and $J = 0.85$ eV calculated by means of constrained DFT procedure. The auxiliary DMFT impurity problem was solved for the inverse temperature parameter $\beta = 40\,\text{eV}^{-1}$ (corresponds to 290 K). Comparison of orbitally resolved LDA+DMFT spectral functions obtained the present work for stoichiometric NdFeAsO and LaFeAsO is shown in Fig. 4. For both

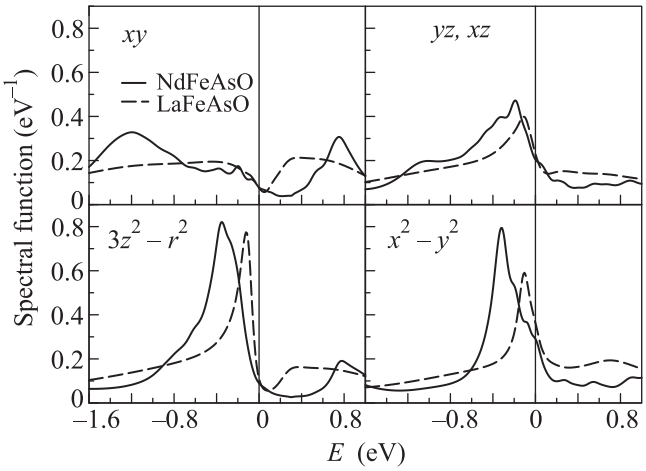

Fig. 4. Spectral functions of NdFeAsO (solid curves) and LaFeAsO (dashed curves) in the vicinity of the Fermi energy (0 eV) obtained within LDA+DMFT

compounds dynamical Coulomb correlations renormalize the spectral functions in the vicinity of the Fermi energy. Quantitative measure of this renormalization is provided by a quasiparticle mass enhancement m^*/m. In the present study it was computed by definition as an inverse of the quasiparticle renormalization factor Z, $m^*/m = Z^{-1} = [1 - \partial \mathrm{Re}\Sigma(\omega)/\partial\omega]|_{\omega=0}$. In the case of LaFeAsO band renormalization is stronger corresponding to the effective quasiparticle mass enhancement $m^*/m \approx 2$ [2, 4] while according to our calculation NdFeAsO is less correlated with $m^*/m \approx 1.4$. In this connection it is instructive to recall other pnictide compound LaFePO where correlations are as strong as in LaFeAsO [6] but the transition temperature is order of magnitude smaller (7 K).

In Fig. 3 we compare our LDA+DMFT results with experimental ARPES data of Liu et al. [16]. Taking into consideration the local dynamical correlations considerably improves the LDA solution. The calculated DMFT spectral function $A(\mathbf{k}, \omega)$ is in good agreement with experimentally measured intensity map. The following features are seen both in theoretical and experimental spectra: the hole pocket centered at the Γ point, the electron pocket centered at the M point, and the flat band in the energy interval $(-0.2, -0.3)$ eV near the Γ point. In addition, there are two bands crossing the Fermi level on both sides of the Γ point on the X–Γ–M direction. However, position of this crossing and the double sheet character of the Fermi surface are different from the experiment. Also the depth of the electron pocket at the M point remains overestimated. As pointed out by authors of the work [16] this disagreement may be connected with surface sensitivity of ARPES.

Unfortunately there is no good ARPES spectra for doped $LaFeAsO_{0.9}F_{0.1}$ to compare with our results for $NdFeAsO_{0.9}F_{0.1}$. However, assuming in first approximation that doping is equivalent to orbital-dependent shift of the bands, we can conclude that band structure of $LaFeAsO_{0.9}F_{0.1}$ should be in general the same as in the neodymium-based compound. The only expected difference is the position of the bands below the Fermi energy. In comparison with $NdFeAsO_{0.9}F_{0.1}$ in fluorine-doped LaFeAsO depth of the electron pocket centered at the M point is expected to be smaller and dome-like band at the Γ point may cross the Fermi level.

In conclusion, by employing the LDA+DMFT computational scheme we investigated the spectral properties of superconducting $NdFeAsO_{0.9}F_{0.1}$. The calculated band structure is in good agreement with the experimental ARPES data. Our calculations show that the band dispersion observed in ARPES cannot be understood within LDA-based approach and dynamical electronic correlations must be explicitly taken into account. We expect that unlike $NdFeAsO_{0.9}F_{0.1}$ the bands at the top of the valence band at the Γ point in $LaFeAsO_{0.9}F_{0.1}$ may cross the Fermi level. Strength of electronic correlations in $NdFeAsO_{0.9}F_{0.1}$ and its parent compound is smaller than in LaFeAsO and LaFePO. Thus, our results demonstrate that there is no direct connection between the critical temperature and the correlation strength in the pnictides.

This work was supported by the Russian Foundation for Basic Research (Projects # 13-02-00050, 12-02-31207-mol_a, 12-02-91371-CT_a) and The Ministry of education and science of Russian Federation, project 14.A18.21.0076. The authors acknowledge the support from the Ural Branch of the Russian Academy of Sciences, grants 12-T-3-1003 and 12-П-3-1015. S.L.S. is grateful to the Dynasty Foundation. S.L.S and V.I.A. are grateful to the Center for Electronic Correlations and Magnetism, University of Augsburg for hospitality. Support by the Deutsche Forschergemeinschaft through FOR 1346 (S.L.S.) is gratefully acknowledged.

1. Y. Kamihara, H. Hiramatsu, M. Hirano et al., J. Am. Chem. Soc. **128**, 10012 (2006).
2. V. I. Anisimov, Dm. M. Korotin, M. A. Korotin et al., J. Phys.: Condens. Matter **21**, 075602 (2009).
3. K. Haule, J. H. Shim, and G. Kotliar, Phys. Rev. Lett. **100**, 226402 (2008).
4. M. Aichhorn, L. Pourovskii, V. Vildosola et al., Phys. Rev. B **80**, 085101 (2009).
5. S. L. Skornyakov, A. V. Efremov, N. A. Skorikov et al., Phys. Rev. B **80**, 092501 (2009).

6. S. L. Skornyakov, N. A. Skorikov, A. V. Lukoyanov et al., Phys. Rev. B **81**, 174522 (2010).
7. M. V. Sadovskii, E. Z. Kuchinskii, and I. A. Nekrasov, J. Magn. Magn. Mater. **324**, 3481 (2012).
8. I. A. Nekrasov, Z. V. Pchelkina, and M. V. Sadovskii, JETP Lett. **88**(2), 144 (2008).
9. M. V. Sadovskii, Phys.-Usp. **51**, 1201 (2008).
10. S. L. Skornyakov, A. A. Katanin, and V. I. Anisimov, Phys. Rev. Lett. **106**, 047007 (2011); S. L. Skornyakov, V. I. Anisimov, and D. Vollhardt, Phys. Rev. B **86**, 125124 (2012).
11. Z. A. Ren, J. Yang, W. Lu et al., Materials Research Innovations **12**(3), 105 (2008).
12. K. Kuroki, H. Usui, S. Onari et al., Phys. Rev. B **79**, 224511 (2009).
13. D. H. Lu, M. Yi, S.-K. Mo et al., Physica C **469**, 452 (2009).
14. L. X. Yang, B. P. Xie, Y. Zhang et al., Phys. Rev. B **82**, 104519 (2010).
15. C. Liu, Y. Lee, A. D. Palczewski et al., Phys. Rev. B **82**, 075135 (2010).
16. C. Liu, T. Kondo, A. D. Palczewski et al., Physica C **469**, 491 (2009).
17. T. Kondo, A. F. Santander-Syro, O. Copie et al., Phys. Rev. Lett. **101**, 147003 (2008).
18. V. I. Anisimov, A. I. Poteryaev, M. A. Korotin et al., J. Phys.: Condens. Matter **9**, 7359 (1997); K. Held, I. A. Nekrasov, G. Keller et al., Phys. Stat. Sol. B **243**, 2599 (2006).
19. W. Metzner and D. Vollhardt, Phys. Rev. Lett. **62**, 324 (1989).
20. Y. Kamihara, T. Watanabe, M. Hirano, and H. Hosono, J. Am. Chem Soc. **130**, 3296 (2008).
21. Z.-A. Ren, J. Yang, W. Lu et al., Europhys. Lett. **82**, 57002 (2008).
22. A. Koitzsch, D. Inosov, J. Fink et al., Phys. Rev. B **78**, 180506 (2008).
23. K. Kuroki, H. Usui, S. Onari et al., Phys. Rev. B **79**, 224511 (2009).
24. P. H. Dederichs, S. Blügel, R. Zeller, and H. Akai, Phys. Rev. Lett. **53**, 2512 (1984); O. Gunnarsson, O. K. Andersen, O. Jepsen, and J. Zaanen, Phys. Rev. B **39**, 1708 (1989); V. I. Anisimov and O. Gunnarsson, Phys. Rev. B **43**, 7570 (1991).
25. http://elk.sourceforge.net/.
26. Y. Qiu, W. Bao, Q. Huang et al., Phys. Rev. Lett. **101**, 257002 (2008).
27. V. I. Anisimov, D. E. Kondakov, A. V. Kozhevnikov et al., Phys. Rev. B **71**, 125119 (2005).
28. P. Werner, A. Comanac, L. de' Medici et al., Phys. Rev. Lett. **97**, 076405 (2006).
29. A. I. Liechtenstein, V. I. Anisimov, and J. Zaanen, Phys. Rev. B **52**, R5467 (1995).
30. J. H. Vidberg and J. E. Serene, J. Low Temp. Phys. **29**, 179 (1997).